Physics

Light & Optics fields

Okayama University *Year* 2005

Sound velocity and multibranch bogoliubov spectrum of an elongated fermi superfluid in the BEC-BCS crossover

Tarun Kanti Ghosh
Okayama University

Kazushige Machida
Okayama University

Sound velocity and multibranch Bogoliubov spectrum of an elongated Fermi superfluid in the BEC-BCS crossover

Tarun Kanti Ghosh and Kazushige Machida
Department of Physics, Okayama University, Okayama 700-8530, Japan
(Received 7 October 2005; published 12 January 2006)

We study properties of excited states of an elongated Fermi superfluid along the Bose-Einstein-condensate–BCS crossover including the unitarity limit. Analytic expressions for the sound velocity in an inhomogeneous as well as homogeneous Fermi superfluid along the crossover are obtained on the basis of the hydrodynamic theory. The complete excitation spectrum of axial quasiparticles with various discrete radial nodes is presented. We discuss the feasibility of measuring the sound velocity and the multibranch Bogoliubov spectrum experimentally.

DOI: 10.1103/PhysRevA.73.013613 PACS number(s): 03.75.Kk, 03.75.Ss, 32.80.Lg

I. INTRODUCTION

Strongly interacting two-component Fermi gases provide a unique testing ground for the theories of exotic systems in nature. In atomic Fermi gases, tunable strong interactions are produced using the Feshbach resonance [1–3]. By sweeping the magnetic field in Feshbach resonance experiments, the magnitude and nature of the two-body interaction strength changes from repulsive to attractive. Across the resonance the *s*-wave scattering length a goes from large positive to large negative values. The fermionic system becomes molecular Bose-Einstein condensates (BEC's) for strong repulsive interaction and transforms into the Bardeen-Cooper-Schrieffer (BCS) superfluid when the interaction is attractive. The first observations of the BEC's of molecules consisting of loosely bound fermionic atoms [5–7] initiated a series of explorations [4,8–11] of the crossover between BEC and BCS superfluid. The size of fermion pair condensates smoothly increases from the BEC to the BCS side of the resonance. Near the resonance, the zero-energy *s*-wave scattering length a exceeds the interparticle spacing and the interparticle interactions are unitarity limited and universal. Recent experiments have entered the crossover regime and yielded results of the interaction strength by measuring the cloud size and expansion.

As in the case of bosonic clouds the frequencies of collective modes of Fermi gases can be measured to high accuracy, it is of major interest to investigate their dependence on the equation of state along the crossover. It was pointed out [12] that the collective frequencies of a superfluid Fermi gas at $T=0$, trapped in a harmonic potential, approach well-defined values in the BEC and the unitarity limit regimes, where the density dependence of the chemical potential can be inferred from general arguments. In the intermediate region, various investigations, based on the hydrodynamic theory of superfluid and suitable parametrizations of the equation of state, have appeared recently [13–19]. The first experimental results on the collective frequencies of the lowest axial and radial breathing modes on ultracold gases of ^{6}Li across the Feshbach resonance have also become available [20,21]. Since the BCS and the unitarity limits are characterized by the same collective excitation frequencies, there is a growing interest to study the sound velocity [22–24] to make a clear identification of these two regimes and to better characterize two kinds of superfluid.

The axial excitations of ultracold gases in a cigar-shaped trap can be divided into two regimes: (i) long-wavelength excitations where the wavelength is equal to or larger than the axial size and (ii) short-wavelength excitations where the wavelength is much smaller than the axial size. In the former case, the axial excitations are discrete and the lowest breathing-mode frequency has been measured [20,21]. In the latter case, the axial excitations can be described by a continuous wave vector k. However, the finite transverse size of the system also produces a discreteness in the radial spectrum. The short-wavelength axial phonons with a different number of discrete radial nodes give rise to the multibranch Bogoliubov spectrum (MBS) [25].

The inhomogeneous density in the radial plane determines the curvature of the mode spectrum. The effect of the inhomogeneous density in the radial plane decreases (since the radial size increases) as we go from the molecular BEC side to the weak-coupling BCS side for a fixed number of atoms and the trapping potential. We would expect that the MBS will be different in the different regimes and it can be used to distinguish different superfluid regimes along the BEC-BCS crossover.

It should be noted that the axial excited state is coupled with the discrete radial nodes within a given angular momentum symmetry. For example, when we excite the system to study the sound propagation along the symmetry axis, this perturbation inherently excites all other low-energy transverse modes having zero angular momentum. Similarly, the above arguments are also applicable to other low-energy mode spectra—e.g, the spectrum for the breathing mode. To determine the various mode spectra, we must take into account the incidence of mode coupling between the axial quasiparticle states and the transverse modes.

In this work, we calculate the sound velocity in an inhomogeneous as well as homogeneous Fermi superfluid along the BEC-BCS crossover. We also study the low-energy MBS of a cigar-shaped superfluid Fermi gas along the BEC-BCS crossover by including the mode coupling. It is important to study such a spectrum in view of the current Bragg scattering

experiment [26] on the MBS of an elongated cloud of a weakly interacting BEC.

This paper is organized as follows. In Sec. II, we calculate the transverse eigenfrequencies and its corresponding eigenfunction of an elongated Fermi superfluid along the BEC-BCS crossover. In Sec. III, we discuss the equation of state of the Fermi superfluid. The sound-velocity, phonon-mode, and monopole-mode spectra are presented in Sec. IV. We give a brief summary and conclusions in Sec. V.

II. HYDRODYNAMIC EQUATIONS AND EIGENFREQUENCIES

We consider a two-component Fermi gas in a long cigar-shaped harmonic trap potential $V(r,z)=(M/2)(\omega_r^2 r^2+\omega_z^2 z^2)$ at zero temperature. Here, $\omega_z \ll \omega_r$. We assume that the system behaves hydrodynamically throughout all regimes. If the system is BCS superfluid, then as long as the oscillation frequency is below the gap frequency needed to break up a Cooper pair, this condition is expected to be fulfilled. The system can be described by the Schrödinger equation [16]

$$i\hbar\frac{\partial\psi}{\partial t}=\left[-\frac{\hbar^2}{2M}\nabla^2+V(r)+\mu(n)\right]\psi, \tag{1}$$

where M is the mass of the Fermi particles and $\mu(n)$ is the equation of state which depends on the magnitude and nature of the interaction strength.

Using the Madelung transformation $\psi=\sqrt{n}e^{i\theta}$ and neglecting the quantum pressure term, we obtain the hydrodynamic equations of motion for the Fermi superfluid which are given by the continuity and the Euler equations, respectively,

$$\frac{\partial n}{\partial t}=-\nabla\cdot[n\mathbf{v}] \tag{2}$$

and

$$M\frac{\partial\mathbf{v}}{\partial t}=-\nabla\left[\mu(n)+V(r)+\frac{1}{2}M\mathbf{v}^2\right]. \tag{3}$$

Here, $n(\mathbf{r},t)$ and $\mathbf{v}(\mathbf{r},t)=(\hbar/M)\nabla\theta$ are the local density and superfluid velocity, respectively. We also assumed that $\omega_r \gg \omega_z$ so that it makes a long cigar-shaped trap.

The equation of state enters through the density-dependent chemical potential. We assume the power-law form of the equation of state as $\mu(n)=Cn^\gamma$ as in Refs. [13–15,17,19]. At equilibrium, the density profile takes the form $n_0(r)=(\mu/C)^{1/\gamma}(1-\tilde{r}^2)^{1/\gamma}$, where $\tilde{r}=r/R$, and $R=\sqrt{2\mu/M\omega_r^2}$. Linearizing around equilibrium, $n=n_0+\delta n$, $\mathbf{v}=\delta\mathbf{v}$, and $\mu(n)=\mu(n_0)+(\partial\mu/\partial n)|_{n=n_0}\delta n$. The equations of motion for the density and velocity fluctuations are

$$\frac{\partial\delta n}{\partial t}=-\nabla\cdot[n_0(r)\delta\mathbf{v}], \tag{4}$$

$$M\frac{\partial\delta\mathbf{v}}{\partial t}=-\nabla\left[\left.\frac{\partial\mu(n)}{\partial n}\right|_{n=n_0}\delta n\right]. \tag{5}$$

Taking the first-order time derivative of Eq. (4) and using Eq. (5), the second-order equation of motion for the density fluctuation is given by

$$\frac{\partial^2\delta n}{\partial t^2}=\nabla\cdot\left[n_0(r)\nabla\left.\frac{\partial\mu(n)}{\partial n}\right|_{n=n_0}\delta n\right]. \tag{6}$$

In the long cigar-shaped trap, we assume the normal-mode solution of the density fluctuation which can be written as

$$\delta n(r,z,t)=\delta n(r)e^{i[\omega(k)t-kz]}. \tag{7}$$

Substituting Eq. (7) into Eq. (6), then one can obtain

$$-\tilde{\omega}_\alpha^2(k)\delta n(r)=\frac{\gamma}{2}\nabla_{\tilde{r}}\cdot[(1-\tilde{r}^2)^{1/\gamma}\nabla_{\tilde{r}}(1-\tilde{r}^2)^{1-1/\gamma}\delta n(r)]-\frac{\gamma}{2}\tilde{k}^2(1-\tilde{r}^2)\delta n(r), \tag{8}$$

where $\tilde{\omega}=\omega/\omega_r$ and $\tilde{k}=kR$. Here, α is a set of two quantum numbers: the radial quantum number n_r and the angular quantum number m.

For $k=0$, it reduces to a two-dimensional eigenvalue problem and the solutions of it can be obtained analytically. The energy spectrum is given by

$$\tilde{\omega}_\alpha^2=|m|+2n_r[\gamma(n_r+|m|)+1]. \tag{9}$$

The corresponding normalized eigenfunction is given by

$$\delta n_\alpha=A(1-\tilde{r}^2)^{1/\gamma-1}\tilde{r}^{|m|}P_{n_r}^{(1/\gamma-1,|m|)}(2\tilde{r}^2-1)e^{im\phi}, \tag{10}$$

where $P_n^{(a,b)}(x)$ is a Jacobi polynomial of order n and ϕ is the polar angle. Also, the normalization constant A is given by

$$A^2=\frac{2^{2-2/\gamma}}{\sqrt{\pi}R^2}\frac{[\Gamma(n_r+1)]^2\Gamma(1/\gamma)\Gamma(2/\gamma+2n_r+|m|)}{\Gamma(1/\gamma-1/2)[\Gamma(1/\gamma+n_r)]^2\Gamma(2n_r+|m|+1)}. \tag{11}$$

For $\gamma=1$, the above energy spectrum and its corresponding eigenfunction exactly match with results of Ref. [27]. Note that the modes with $n_r=0$ and $m\neq 0$ do not depend on the equation of state. This is because the flow in these modes is incompressible and the internal energy does not change during the oscillation period. The radial breathing mode is $\omega_1=\sqrt{2(\gamma+1)}\omega_r$ which exactly matches with the result of Ref. [14]. The experimental results of the radial breathing mode [20,21] are well described [14] by this analytic spectrum.

The solution of Eq. (8) can be obtained for an arbitrary value of k by numerical diagonalization. For $k\neq 0$, we expand the density fluctuation as

$$\delta n=\sum_\alpha b_\alpha\delta n_\alpha(r,\phi). \tag{12}$$

Substituting the above expansion into Eq. (8), we obtain

$$0=\left[\tilde{\omega}_\alpha^2-\{|m|+2n_r[\gamma(n_r+|m|)+1]\}-\frac{\gamma}{2}\tilde{k}^2\right]b_\alpha+\frac{\gamma}{2}\tilde{k}^2\sum_{\alpha'}M_{\alpha\alpha'}b_{\alpha'}. \tag{13}$$

Here, the matrix element $M_{\alpha\alpha'}$ is given by

$$M_{\alpha\alpha'} = A^2 \int d^2\tilde{r}(1-\tilde{r}^2)^2 \gamma_0 \tilde{r}^{2+|m|+|m'|} e^{i(m-m')\phi} \times P_{n_r'}^{(\gamma_0,|m'|)}(2\tilde{r}^2-1) P_{n_r}^{(\gamma_0,|m|)}(2\tilde{r}^2-1), \quad (14)$$

where $\gamma_0 = 1/\gamma - 1$. The above eigenvalue problem [Eq. (13)] is block diagonal with no overlap between the subspaces of different angular momenta, so that the solutions to Eq. (13) can be obtained separately in each angular momentum subspace. We can obtain all low-energy multibranch Bogoliubov spectra on both sides of the Feshbach resonance including the unitarity limit from Eq. (13) which is our main result. Equations (13) and (14) show that the spectrum depends on the average over the radial coordinate and the coupling between the axial mode and transverse modes within a given angular momentum symmetry. Particularly, the coupling is important for large values of k.

III. EQUATION OF STATE

To calculate the sound velocity and the MBS, we need to know how the adiabatic index γ depends on the two-body interaction strength. At zero temperature, the energy per particle of a dilute Fermi system can be written as

$$\epsilon = \frac{3}{5} E_F \epsilon(y), \quad (15)$$

where $E_F = \hbar^2 k_F^2 / 2M$ is the free-particle Fermi energy and $\epsilon(y)$ is a function of the interaction parameter $y = 1/k_F a$. In the unitarity limit ($y \to 0^{\pm}$) one expects that the energy per particle is proportional to that of a noninteracting Fermi gas. The fixed-node diffusion Monte Carlo calculation of Astrakharchik *et al.* [28] finds $\epsilon(y \to 0) = 0.42 \pm 0.01$. An analogous calculation of Carlson *et al.* [29] gave $\epsilon(y \to 0) = 0.44 \pm 0.01$. The calculation of Astrakharchik *et al.* [28] is quite complete and gives the behavior of the energy of the system across the unitarity limit. On the basis of the data of Carlson *et al.* [29], Bulgac and Bertsch [15] proposed the following behavior of $\epsilon(y)$ near the unitarity limit:

$$\epsilon(y) = \xi - \zeta y - \frac{5}{3} y^2 + O(y^3), \quad (16)$$

where $\xi \sim 0.44$ and $\zeta = 1$ for both positive and negative values of y. However, the data of Ref. [28] give a continuous but not differentiable behavior of $\epsilon(y)$ near $y = 0$ and they suggest $\zeta = \zeta_- = 1$ in the BCS regime and $\zeta = \zeta_+ = 1/3$ in the BEC regime. On the basis of the data of Astrakharchik *et al.* [28], Manini and Salasnich [17] proposed the following analytical fitting formula of $\epsilon(y)$ for all regimes in the BEC-BCS crossover including the unitarity limit:

$$\epsilon(y) = \alpha_1 - \alpha_2 \tan^{-1}\left[\alpha_3 y \frac{\beta_1 + |y|}{\beta_2 + |y|} \right]. \quad (17)$$

This analytical expression is well fitted with the data of Ref. [28] for a wide range of y on both sides of the resonance. We shall use Eq. (17) for further studies in this work. Two different sets of parameters are considered in Ref. [17]: one set in the BCS regime ($y < 0$) and another set in the BEC regime ($y > 0$). In the BCS limit, the values of the parameters [17] are $\alpha_1 = 0.42$, $\alpha_2 = 0.3692$, $\alpha_3 = 1.044$, $\beta_1 = 1.4328$, and $\beta_2 = 0.5523$. In the BEC limit, the values of the parameters [17] are $\alpha_1 = 0.42$, $\alpha_2 = 0.2674$, $\alpha_3 = 5.04$, $\beta_1 = 0.1126$, and $\beta_2 = 0.4552$. The advantage of a functional parametrization of $\epsilon(y)$ is that it allows straightforward analytical calculations of several physical properties. The chemical potential μ is given by [17]

$$\mu = \epsilon(n) + n \frac{d\epsilon(n)}{dn} = E_F \left[\epsilon(y) - \frac{y}{5} \epsilon'(y) \right], \quad (18)$$

where $\epsilon'(y) = \partial \epsilon(y) / \partial y$. One can extract an effective adiabatic index γ and its dependence on the scattering length a by defining the logarithmic derivative as [17]

$$\gamma \equiv \bar{\gamma} = \frac{n}{\mu} \frac{d\mu}{dn} = \frac{\frac{2}{3} - \frac{2y}{5}\epsilon'(y) + \frac{y^2}{15}\epsilon''(y)}{\epsilon(y) - \frac{y}{5}\epsilon'(y)}. \quad (19)$$

The radial size of the Fermi system in all regimes of the BEC-BCS crossover can be obtained from the relation $R = \sqrt{2\mu / M\omega_r^2}$. From Eq. (18), one can obtain the radial size which is given by

$$R = r_0 \sqrt{\epsilon(y) - \frac{y}{5}\epsilon'(y)}, \quad (20)$$

where $r_0 = a_{\mathrm{av}}(24N)^{1/6}$ is the radial size of the free Fermi gas in a harmonic trap potential [30,31], $a_{\mathrm{av}} = \sqrt{\hbar / M\omega_{\mathrm{av}}}$, and $\omega_{\mathrm{av}} = (\omega_r^2 \omega_z)^{1/3}$ is the average oscillator frequency of the trap potential. In the weak-coupling BCS limit, the ground-state energy per particle is $\epsilon_{\mathrm{bcs}}(n) = (3/5)E_F$ and the chemical potential is $\mu_{\mathrm{bcs}} = E_F$. The corresponding radius is $R_{\mathrm{bcs}} = a_{\mathrm{av}}(24N)^{1/6} = r_0$. In the unitarity limit, the ground-state energy per particle is $\epsilon_{\mathrm{uni}}(n) = (3/5)E_F \xi$ and the chemical potential is $\mu_{\mathrm{uni}} = E_F \xi$. The corresponding radius is $R_{\mathrm{uni}} = a_{\mathrm{av}}(24N\xi^3)^{1/6} = r_0\sqrt{\xi}$.

IV. SOUND VELOCITY AND MULTIBRANCH BOGOLIUBOV SPECTRUM

A. Sound velocity

Before presenting the exact numerical results, we make some approximation for a quantitative discussion. If we neglect the couplings among all other modes in the $m = 0$ sector by setting $l' = (n_r, 0)$ in Eqs. (13) and (14), one can easily get following spectrum:

$$\tilde{\omega}_{n_r}^2 = 2n_r(\gamma n_r + 1) + \frac{\gamma}{2}(1 - M_{n_r,n_r})\tilde{k}^2. \quad (21)$$

In the limit of long wavelength, the $n_r = 0$ mode is phonon like with a sound velocity

$$u_1 = \sqrt{\frac{(2-\gamma)\gamma}{2}\frac{\mu}{M}}. \tag{22}$$

For $\gamma=1$, it exactly reproduces the weakly interacting BEC results [25]. This sound velocity is different from the result obtained in Ref. [24]. The reason for the difference is given below. In Ref. [24], the sound velocity is obtained by simply integrating Eq. (8) on radial coordinates. In this work, we are multiplying by the complex conjugate of δn on both sides of Eq. (8) and then integrating it on radial coordinates. Since the density fluctuation at the lowest-energy state is a function of the radial coordinate, the two average procedures give two different results. Note that the correct average procedure is considered in our work. For the homogeneous Fermi system, the sound velocity can be obtained from Eq. (21) by neglecting M_{n_r,n_r} and it is given by

$$u_1 = \sqrt{\frac{\gamma\mu}{M}}. \tag{23}$$

The sound velocity in the inhomogeneous system is smaller by a factor of $\sqrt{1-\gamma/2}$ with respect to the sound velocity in a homogeneous Fermi system. This is due to the effect of the average over the radial variable which can be seen from Eqs. (13) and (14).

Using Eqs. (18), (19), and (22), the sound velocity in the inhomogeneous Fermi superfluid along the BEC-BCS crossover including the unitarity limit is given by

$$u_1 = v_F \sqrt{\frac{\left[\frac{1}{3}-\frac{y}{5}\epsilon'(y)+\frac{y^2}{30}\epsilon''(y)\right]\left[-\frac{1}{3}+\epsilon(y)-\frac{y^2}{30}\epsilon''(y)\right]}{\left[\epsilon(y)-\frac{y}{5}\epsilon'(y)\right]}}, \tag{24}$$

where $v_F=\sqrt{2E_F/M}$ is the Fermi velocity. Similarly, by using Eqs. (18), (19), and (23), the sound velocity in the homogeneous Fermi superfluid along the BEC-BCS crossover including the unitarity limit is given by

$$u_1 = v_F \sqrt{\frac{1}{3}\epsilon(y)-\frac{y}{5}\epsilon'(y)+\frac{y^2}{30}\epsilon''(y)}. \tag{25}$$

Equation (25) exactly agrees with the result of Ref. [17].

In the molecular BEC limit, the sound velocity in the inhomogeneous bosonic systems can be written as $u_m=\sqrt{\mu_m/2M_m}$, where μ_m is the chemical potential of the molecular BEC and $M_m=2M$ is the mass of a molecule. The chemical potential μ_m can be written as $\mu_m=4\pi a_m\hbar^2 n_m/M_m$, where $n_m=k_F^3/6\pi^2$ is the molecular density and k_F is the Fermi wave vector. Here, $a_m=0.6a$ is the two-body scattering length between two bound molecules [32]. A simple expression for the sound velocity in the molecular BEC limit can be written as

$$u_m = v_F \sqrt{\frac{0.6}{12\pi}\frac{1}{y}}. \tag{26}$$

Using Eqs. (24)–(26), we plot the sound velocity along the BEC-BCS crossover in Fig. 1. There is a small kink at the unitarity limit $y=0$ due to $\zeta_-\neq\zeta_+$. Otherwise, Fig. 1 shows that there is a smooth crossover of the sound velocity from the molecular BEC side to the BCS side through the unitarity limit $y=0$. Figure 1 also shows that Eq. (26) matches very well with Eq. (24) for large values of y.

For homogeneous Fermi systems the sound velocity in the two limiting cases can be obtained from Eq. (25) and these are given by $u_1=0.37v_F$ in the unitarity limit and by $u_1=0.57v_F$ in the weak-coupling BCS limit. These results exactly match the previous results [22,23]. Similarly, the sound velocity for the inhomogeneous Fermi systems in the two limiting cases can be obtained from Eq. (24) and these are given by $u_1=0.30v_F$ in the unitarity limit and $u_1=0.45v_F$ in the dilute BCS limit. The sound velocity in the inhomogeneous Fermi system is less than that in the homogeneous Fermi system with the same density at the center of the trap as the former system. However, this difference is large in the BCS side compared to the BEC side. The sound velocity of the inhomogeneous Fermi superfluid can be measured by observing the propagation of the sound pulses along

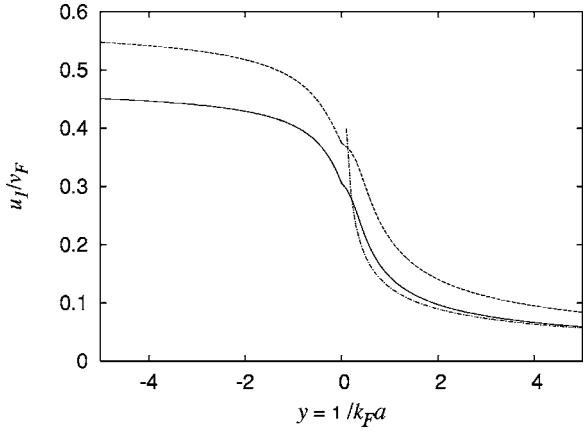

FIG. 1. Plots of the sound velocity along the BEC-BCS crossover including the unitarity limit. The solid and dashed lines are corresponding to the sound velocity in inhomogeneous and homogeneous Fermi superfluid, respectively. The dot-dashed line corresponds to Eq. (26).

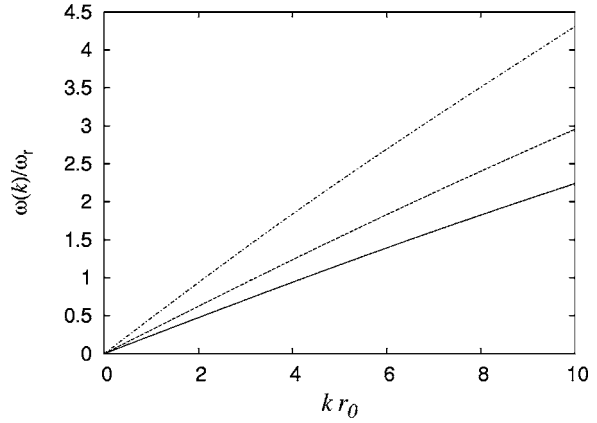

FIG. 2. Plots of the phonon-mode spectrum in the BCS limit (dot-dashed line), unitarity limit (dashed line), and BEC side of the unitarity limit with $y=0.25$ (solid line).

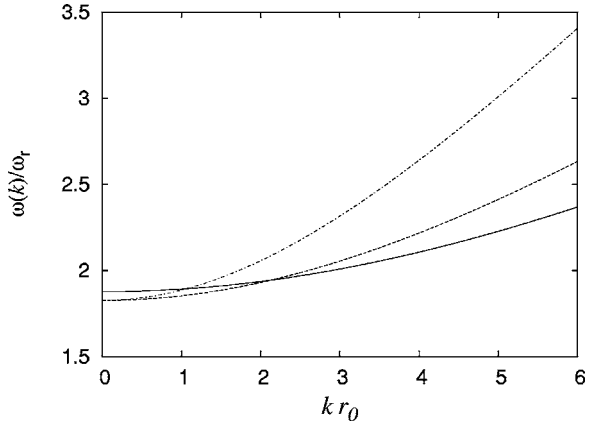

FIG. 3. Plots of the monopole-mode spectrum in the BCS limit (dot-dashed line), unitarity limit (dashed line), and BEC side of the unitarity limit with $y=0.25$ (solid line).

the symmetry axis as is done for weakly interacting BEC's [33].

B. Phonon-mode spectrum

In Fig. 2 we plot the phonon-mode spectrum in the weak-coupling BCS limit ($y \ll 0$), unitarity limit ($y=0$) and BEC side of the unitarity limit ($y=0.25$) by solving Eq. (13). These spectra have the usual form like $\omega=u_1 k$ at low momenta, where the sound velocity u_1 is given in Eq. (24). It is seen from Fig. 2 that the behavior of the phonon-mode spectrum is different for different regimes characterizing each superfluid phase. For example, the slope of the phonon spectrum in the BCS limit is large compared to the unitarity and BEC limits as expected.

C. Monopole-mode spectrum

In Fig. 3, we plot the monopole-mode spectrum in three different regimes by solving Eq. (13). In the long-wavelength limit, the monopole mode has the free-particle dispersion relation with some effective mass m_b and a gap $\Delta_b=\sqrt{2(\gamma+1)}\omega_r$. In the long-wavelength limit, the breathing-mode spectrum can be calculated from Eq. (13) by using first-order perturbation theory. The spectrum for the monopole mode in the long-wavelength limit is given by $\omega_1(k)=\sqrt{2(\gamma+1)}\omega_r+\hbar k^2/2m_b+O(k^4)$, where the effective mass of the breathing mode m_b is

$$m_b = M\frac{\hbar\omega_r}{\mu}\sqrt{\frac{8}{\gamma^2}\frac{(2+\gamma)(\gamma+1)}{(2-\gamma)^2}}. \tag{27}$$

Note that $\gamma=2/3$ in the BCS and unitarity limits. Therefore, the monopole-mode frequencies are the same at the BCS and the unitarity limits. However, the behaviors of the spectrum in two different regimes are completely different. For example, the effective mass of the monopole mode spectrum in the BCS limit is small compared to that of the unitarity limit.

V. SUMMARY AND CONCLUSIONS

In this work, we have calculated the sound velocity in the homogeneous as well as inhomogeneous Fermi superfluid along the BEC-BCS crossover. The sound velocity in the inhomogeneous Fermi superfluid can be measured by observing the sound pulse propagation along the symmetry axis, similar to the experiment by Andrews *et al.* [33] for weakly interacting BEC's. The hydrodynamic description presented in this work enables us to produce correctly all low-energy multibranch Bogoliubov spectra by including the coupling of the axial mode with the radial modes within the same angular momentum sector. An analytic expression for the effective mass of the breathing-mode spectrum is obtained. Due to the axial symmetry, the modes having zero angular momentum can be excited in the Bragg scattering experiment. Particularly, the spectra for the phonon and monopole modes in the different regimes can be observed in the Bragg scattering experiments as these spectra are observed in Ref. [26] for weakly interacting BEC's. By measuring the sound velocity in the pulse propagation experiment and by observing the low-energy Bogoliubov spectrum in the Bragg spectroscopy, one can make a clear identification of various superfluid regimes along the BEC-BCS crossover.

ACKNOWLEDGMENTS

This work of T.K.G. was supported by a grant (Grant No. P04311) of the Japan Society for the Promotion of Science.

[1] M. Houbiers, H. T. C. Stoof, W. I. McAlexander, and R. G. Hulet, Phys. Rev. A **57**, R1497 (1998).
[2] W. C. Stwalley, Phys. Rev. Lett. **37**, 1628 (1976).
[3] E. Tiesinga, B. J. Verhaar, and H. T. C. Stoof, Phys. Rev. A **47**, 4114 (1993).
[4] K. M. O'Hara, S. L. Hemmer, M. E. Gehm, S. R. Grande, and J. E. Thomas, Science **298**, 217 (2002).
[5] M. Greiner, C. A. Regal, and D. S. Jin, Nature (London) **426**, 537 (2003).
[6] S. Jochim, M. Bartenstein, A. Altmeyer, G. Hendl, S. Riedl, C.

Chin, J. Hecker Denschlag, and R. Grimm, Science **302**, 2101 (2003).
[7] M. W. Zwierlein, C. A. Stan, C. H. Schunck, S. M. F. Raupach, S. Gupta, Z. Hadzibabic, and W. Ketterle, Phys. Rev. Lett. **91**, 250401 (1993).
[8] C. A. Regal, M. Greiner, and D. S. Jin, Phys. Rev. Lett. **92**, 040403 (2004).
[9] M. Bartenstein, A. Altmeyer, S. Riedl, S. Jochim, C. Chin, J. Hecker Denschlag, and R. Grimm, Phys. Rev. Lett. **92**, 120401 (2004).
[10] T. Bourdel, L. Khaykovich, J. Cubizolles, J. Zhang, F. Chevy, M. Teichmann, L. Tarruell, S. J. J. M. F. Kokkelmans, and C. Salomon, Phys. Rev. Lett. **93**, 050401 (2004).
[11] C. Chin, M. Bartenstein, A. Altmeyer, S. Riedl, S. Jochim, J. H. Denschlag, and R. Grimm, Science **305**, 1128 (2004).
[12] S. Stringari, Europhys. Lett. **65**, 749 (2004).
[13] H. Hu, A. Minguzzi, X.-J. Liu, and M. P. Tosi, Phys. Rev. Lett. **93**, 190403 (2004).
[14] H. Heiselberg, Phys. Rev. Lett. **93**, 040402 (2004).
[15] A. Bulgac and G. F. Bertsch, Phys. Rev. Lett. **94**, 070401 (2005).
[16] Y. E. Kim and A. L. Zubarev, Phys. Rev. A **70**, 033612 (2004).
[17] N. Manini and L. Salasnich, Phys. Rev. A **71**, 033625 (2005).
[18] R. Combescot and X. Leyronas, Phys. Rev. Lett. **93**, 138901 (2004).
[19] G. E. Astrakharchik, R. Combescot, X. Leyronas, and S. Stringari, Phys. Rev. Lett. **95**, 030404 (2005).
[20] J. Kinast, S. L. Hemmer, M. E. Gehm, A. Turlapov, and J. E. Thomas, Phys. Rev. Lett. **92**, 150402 (2004).
[21] M. Bartenstein, A. Altmeyer, S. Riedl, S. Jochim, C. Chin, J. H. Denschlag, and R. Grimm, Phys. Rev. Lett. **92**, 203201 (2004).
[22] T. L. Ho, Phys. Rev. Lett. **92**, 090402 (2004).
[23] H. Heiselberg, e-print cond-mat/0409077; e-print cond-mat/0503101.
[24] P. Capuzzi, P. Vignolo, F. Federici, and M. P. Tosi, e-print cond-mat/0509323.
[25] E. Zaremba, Phys. Rev. A **57**, 518 (1998).
[26] J. Steinhauer, N. Katz, R. Ozeri, N. Davidson, C. Tozzo, and F. Dalfovo, Phys. Rev. Lett. **90**, 060404 (2003).
[27] M. Fleesser, A. Csordas, P. Szepfalusy, and R. Graham, Phys. Rev. A **56**, R2533 (1997).
[28] G. E. Astrakharchik, J. Boronat, J. Casulleras, and S. Giorgini, Phys. Rev. Lett. **93**, 200404 (2004).
[29] J. Carlson, S.-Y. Chang, V. R. Pandharipande, and K. E. Schmidt, Phys. Rev. Lett. **91**, 050401 (2003).
[30] S. Y. Chang, V. R. Pandharipande, J. Carlson, and K. E. Schmidt, Phys. Rev. A **70**, 043602 (2004).
[31] D. A. Butts and D. S. Rokhsar, Phys. Rev. A **55**, 4346 (1997).
[32] D. S. Petrov, C. Salomon, and G. V. Shlyapnikov, Phys. Rev. Lett. **93**, 090404 (2004).
[33] M. R. Andrews, D. M. Kurn, H.-J. Miesner, D. S. Durfee, C. G. Townsend, S. Inouye, and W. Ketterle, Phys. Rev. Lett. **79**, 553 (1997).